PII: S0032-3861(97)10089-1

Polymer Vol. 39 No. 21, pp. 4993–5000, 1998
0032-3861/98/$ – see front matter

Reactive compatibilisation of A/(B/C) polymer blends

Part 2. Analysis of the phase inversion region and the co-continuous phase morphology

K. Dedecker and G. Groeninckx*
Katholieke Universiteit Leuven, Department of Chemistry, Laboratory for Macromolecular Structural Chemistry, Celestijnenlaan 200 F, 3001 Heverlee, Belgium
(Accepted 2 September 1997)

The blend polyamide 6 (PA-6)/poly(methyl methacrylate) (PMMA) can be compatibilised by means of the reactive copolymer styrene–maleic anhydride with 20 wt% maleic anhydride (SMA20). The region of phase co-continuity has been analysed for the non-compatibilised and the compatibilised blends with scanning electron microscopy (SEM). The blend composition range of phase co-continuity was shifted to a lower PA-6 content when compatibiliser (SMA20) was added and the co-continuous structures were observed over a much narrower composition range. The effect of the molecular weight of PA-6 on the composition range of phase co-continuity was also analysed; it was found to be shifted to lower PA-6 content with decreasing molecular weight of PA-6. This shift could be interpreted by measuring the melt-viscosity of the different polymers using capillary rheometry. The analysis of the dynamic mechanical properties of the blends confirmed the results obtained with SEM; a clear change in storage modulus (log E') and damping (tan δ) was observed in the phase inversion region. Finally, the crystallisation behaviour of PA-6 in the blends was investigated during cooling from the melt with differential scanning calorimetry. Fractionated crystallisation was observed in the blends where PA-6 forms the dispersed phase.

(Keywords: phase co-continuity; phase inversion; reactive compatibilisation)

INTRODUCTION

The technique of reactive compatibilisation is a very attractive and economical route to achieve stable, multi-phase polymer blends[1]. For most binary polymer blends, the appropriate reactive groups are not present and functionalisation of the blend components is required. However, for some binary polymer blends, a reactive polymer can be added as compatibiliser precursor which is miscible with one of the blend components and reactive towards the other blend component[2]. This strategy is considered in this paper. The compatibilisation of the blend PA-6/PMMA by means of the reactive copolymer SMA has been studied extensively in Part 1[3]. The effect of parameters such as amount and functionality of the compatibiliser, molecular weight of PA-6 and percent dispersed phase on the phase morphology of PA-6/(PMMA/SMA) was studied. In these blends, the matrix consisted of PA-6 and the dispersed particles of PMMA and SMA. In the present paper, the whole composition range is considered for the blend PA-6/(PMMA/SMA20) as well as for the uncompatibilised blend PA-6/PMMA.

In the literature, much attention has been paid to the existence of co-continuous phase morphologies in binary, uncompatibilised blends[4–6]. The effects of viscosity ratio and composition on the phase morphology has been studied for different binary blends[7–9]. However, the effect of compatibilisation on the phase inversion has not been analysed in detail. The phase morphology of the blend system PA-66/PP was studied by Seppälä and co-workers over the whole composition range[10]. The effect of the addition of a compatibiliser (MA-grafted PP) to the blend PA-66/PP on the location and the width of the phase inversion region was investigated but only a minor effect was observed.

EXPERIMENTAL

Materials

The characteristics of the blend components are given in *Table 1*. Two different types of PA-6 were used; they were both provided by DSM-Research. PMMA was provided by Rohm and Haas under the commercial name DIAKON MG-102. SMA20 was supplied by Bayer. The number after SMA denotes the wt% maleic anhydride in SMA. The molecular weight of the polymers were determined using gel-permeation chromatography (GPC) and intrinsic viscosity measurements.

Blend preparation

The blends were prepared in a double screw mini-extruder designed by DSM-Research (The Netherlands) which was described in Part 1[3]. The extrusion temperature was always kept constant at 240°C during blending and the screw speed was 100 rpm. During melt-blending, the mixing chamber was saturated with N_2 gas to avoid oxidative degradation of PA-6 and PMMA[11,12].

The blend components PMMA and SMA20 were premixed during 3 min in order to obtain a miscible blend[13,14]. For the compatibilised blends, the weight ratio PMMA/SMA20 was always 80/20. PA-6 is subsequently

* To whom correspondence should be addressed.

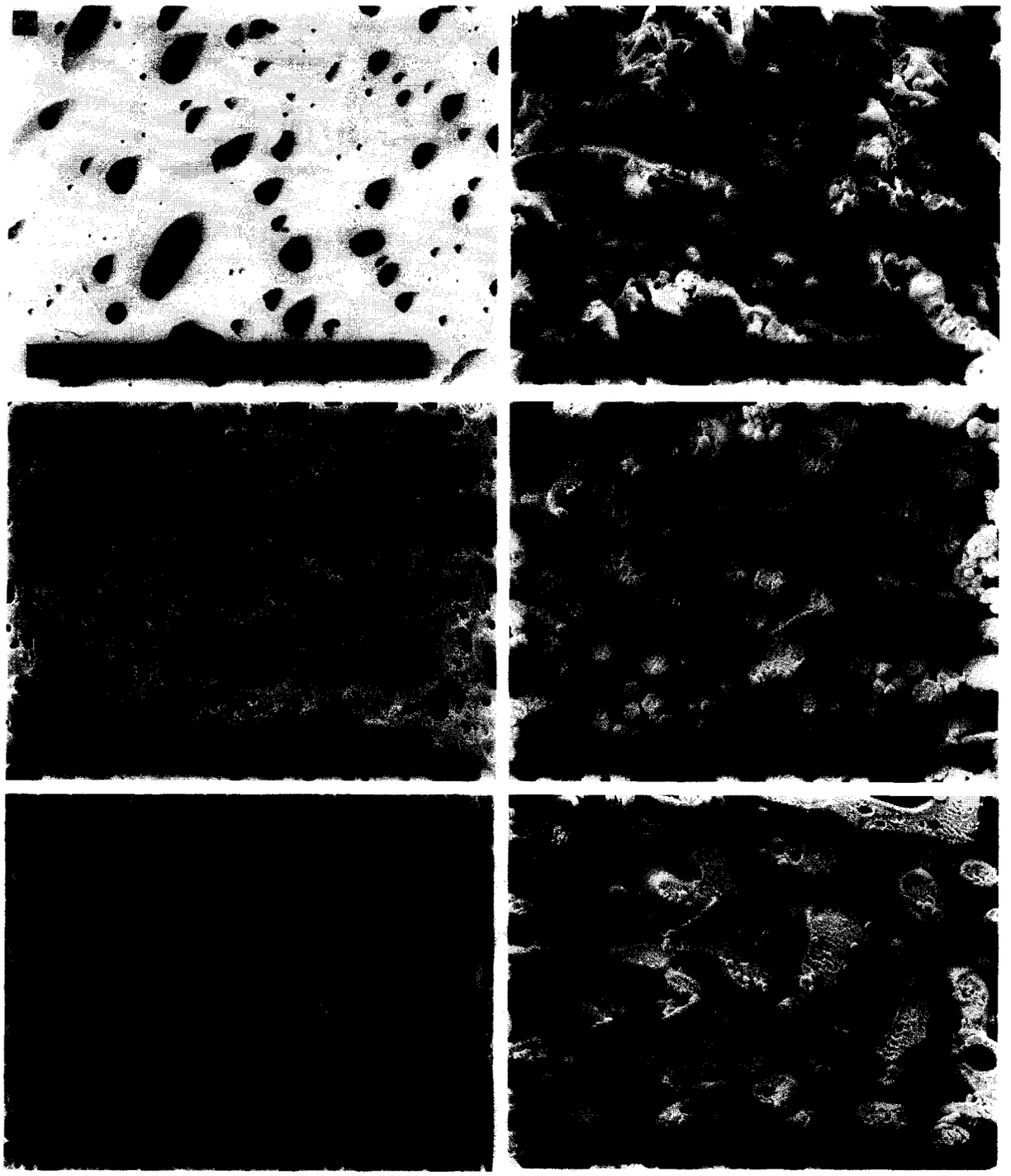

Figure 1 SEM micrographs of the phase morphology of non-compatibilised PA-6/PMMA blends: (1) 70% PA-6; (2) 65% PA-6; (3) 60% PA-6; (4) 55% PA-6; (5) 50% PA-6. (a) Etching with $CHCl_3$; (b) etching with HCl, 6 N

added to this premixed PMMA/SMA20 blend. The blend was melt-mixed during 9 min. After blending, the extruded polymer strand was quenched in a mixture of isopropanol/CO_2 (−78°C) in order to freeze in the phase morphology.

Scanning electron microscopy

The extruded polymer strand was held in liquid N_2 for ±1 min and a brittle fracture was performed. The fracture surface is normally very rough for co-continuous blends. For this reason, the brittle surface was cut at low temperature with a glass knife until a small and flat surface was obtained. This treatment makes the interpretation of the SEM pictures easier.

Two etching methods were used, depending on whether the dispersed phase consisted of PMMA/SMA20 or PA-6. Chloroform was used to dissolve the phase PMMA/SMA20; the etching was performed at room temperature during 48 h. HCl (±6 N) was used as an etching solvent for PA-6; this etching was performed at 85°C during 16 h. In this way, PA-6 is depolymerised into its monomer which is soluble in 6 N HCl[15]. Using this method, the grafted PA-6 chains are also etched away, and in this way a more complete etching of the PA-6 phase is achieved. For blends consisting of a matrix with dispersed particles, etching of the matrix causes a complete disintegration of the blend material and a milky solution is obtained. In this case, only the method to etch

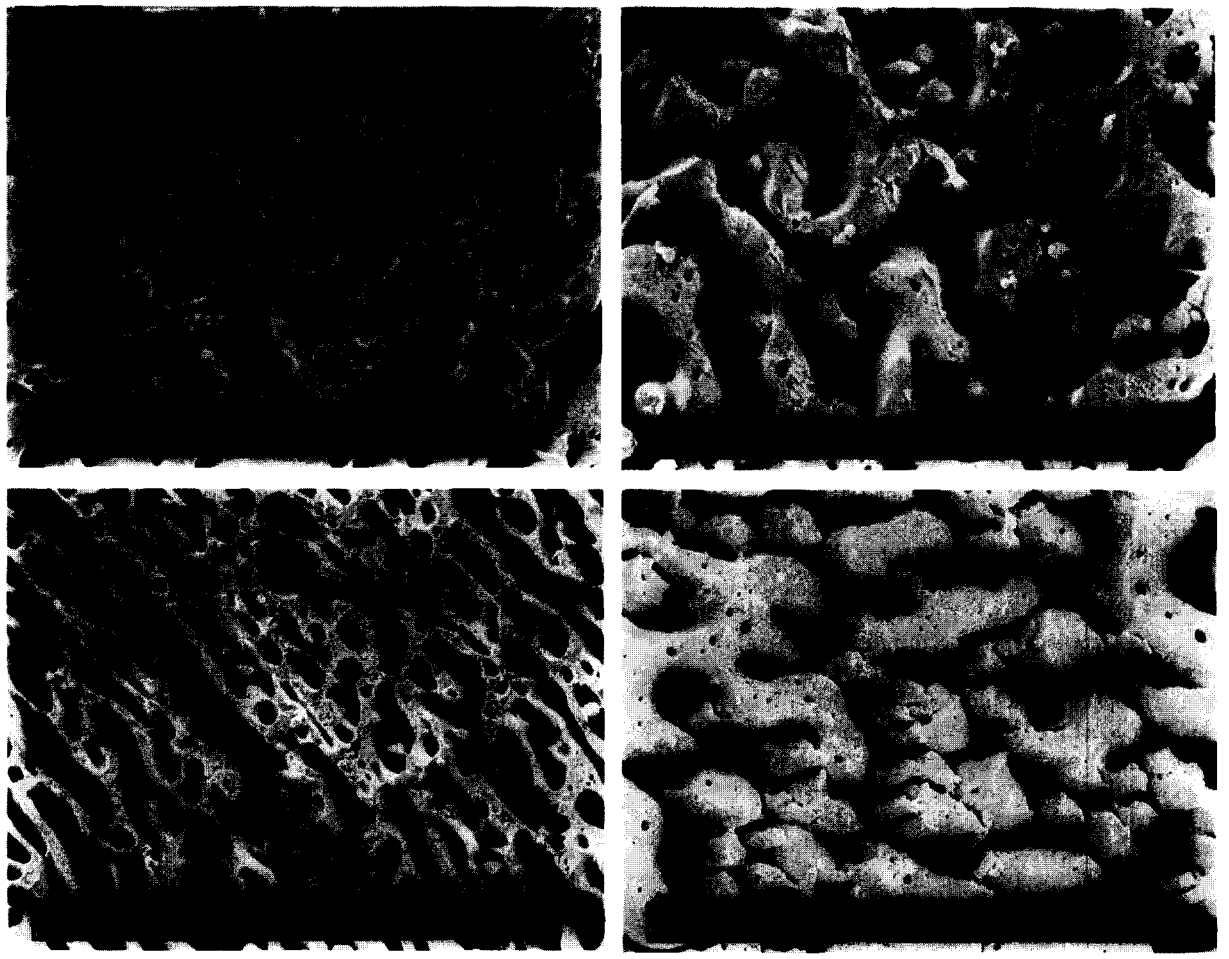

Figure 1 Continued.

Table 1 The molecular characteristics of the different polymers

Material	Method	M_w
PA-6	$[\eta]$ in $HCOOH/H_2O$ 85/15 at 25°C	24000
PA 6		44000
PMMA	GPC in THF	69000
SMA20	$[\eta]$ in THF at 25°C	125000

Table 2 Result of the disintegration tests of the different blend series

	M_w PA-6 = 44 000				M_w PA-6 = 24 000			
	Blend without SMA20		Blend with SMA20		Blend without SMA20		Blend with SMA20	
% PA-6	$CHCl_3$	HCl	$CHCl_3$	HCl	$CHCl_3$	HCl	$CHCl_3$	HCl
20							D	ND
25			D	ND	D	ND	ND	ND
30			D	ND	ND	ND	ND	D
35	D	ND	ND	ND	ND	ND		
40	D	ND	ND	D	ND	ND		
45	D	ND	ND	D	ND	ND		
50	ND	ND	ND	D	ND	ND		
55	ND	ND	ND	D	ND	D		
60	ND	ND	ND	D				
65	ND	ND						
70	ND	ND						
75	ND	D						

D, disintegration; ND, not disintegrated.

away the dispersed phase was used. For some blends, both etching methods could be applied without disintegration of the blend material. This can be seen as an indication of phase co-continuity, as will be discussed later on.

The etched surface was kept under vacuum before coating it with a gold layer of 40 nm. After gold coating, the morphology was examined with a Phillips XL-20 scanning electron microscope.

Capillary rheometry

The Göttfert capillary rheometer was used to measure the melt-viscosity of the polymers as a function of the shear rate. The measurements were performed at 240°C; the polymers were first melted at this temperature for 4 min. The effect of degradation in the capillary rheometer on the viscosity was estimated by measuring the viscosity after different annealing times. The degradation of PA-6 is limited after drying the polymer at 120°C overnight. The viscosity of the different polymers was measured at ±7 different shear rates. The Rabinowitsch correction was applied to the obtained experimental data.

Dynamic mechanical thermal analysis (DMTA)

The extruded polymer strands were compression moulded in order to obtain bars which are suitable for DMTA measurements. The polymer strands were melted at 245°C in a Carver Press during 8 min; then a slight pressure was applied and the heating was turned off. The melted samples were cooled at this low pressure until solid bars were obtained. These bars were sized 30 × 10 × 1 mm^3. The apparatus used is the DMTA M.K. II from Polymer Laboratories. The sample was heated from 30 up to 190°C at a heating rate of 5°C min^{-1}. The applied frequency was 10 Hz.

Differential scanning calorimetry (d.s.c.)

The crystallisation behaviour of the blends was analysed with a DSC-7 from Perkin-Elmer. The samples were heated at 10°C min^{-1} up to 250°C and kept in the melt for 2 min. Subsequently, the samples were cooled from 250 to 50°C at 10°C min^{-1} and a crystallisation curve was obtained.

RESULTS AND DISCUSSION

Location and width of the region of phase co-continuity

It is our goal to study the effect of compatibilisation on the location and width of the region of phase co-continuity. Two series of compatibilised blends, PA-6/(PMMA/SMA20), and two series of non-compatibilised blends, PA-6/PMMA, were prepared. Two different molecular weights of PA-6 were used; for each molecular weight of PA-6, a series of blends without SMA20 and a series of compatibilised blends with a weight ratio PMMA/SMA20 of 80/20 were prepared. For each blend series, all the blend compositions of interest in and around the region of phase co-continuity were considered; the minimum difference in composition between two prepared blends was 5 wt% PA-6. Firstly, the disintegration of the blends in the two etching solvents (HCl, 6 N and $CHCl_3$) was evaluated. When the phase morphology consists of a matrix with dispersed particles, an etching solvent which dissolves the matrix, will cause disintegration of the blend material and a milky solution will be obtained. When both phases are co-continuous, neither of the two etching solvents can cause a complete disintegration of the blend material. The results of these disintegration tests are given in *Table 2*.

As can be seen from *Table 2*, in the series PA-6/PMMA (M_w PA-6 = 44 000), five blend compositions are not disintegrated by $CHCl_3$ nor by HCl, 6 N. Both etching methods could be applied for these five blends with a composition going from 70 to 50% PA-6. The SEM micrographs are presented in *Figure 1*. For the blends with 70, 65 and 60% PA-6, a phase morphology consisting of PMMA particles in a PA-6 matrix is seen after etching with $CHCl_3$. However, a co-continuous phase morphology can be observed for these three blend compositions after applying the etching method with HCl, 6 N. It can clearly be seen that the phase morphology in these three blends consists of a co-continuous network of PMMA rods in the direction of the melt-flow. A two-dimensional view perpendicular to the flow direction after etching away the PMMA phase, gives the wrong impression of a particle–matrix morphology. For the two blends with compositions 55 and 50% PA-6, a co-continuous morphology was observed after applying both etching methods. For the blends with more than 70% PA-6, PMMA particles in a PA-6 matrix can be seen and for the blends with less than 50% PA-6, PA-6 particles in a PMMA matrix are observed.

For the blend series PA-6/(PMMA/SMA20) (M_w PA-6 = 44 000), only one blend composition (35% PA-6) was not disintegrated by $CHCl_3$ or by HCl, 6 N. This can be deduced from *Table 2*. This blend can be considered as co-continuous on the basis of these disintegration tests. However, in *Figure 2*, a PMMA/SMA20 matrix with PA-6 particles is observed after etching with HCl. The etching method with $CHCl_3$ shows a rather complex morphology, which cannot easily be interpreted (*Figure 2*). The morphology of this blend with 35% PA-6 will be discussed further when other techniques (DMTA, d.s.c.) are applied. For the blends with more than 35% PA-6, PMMA/SMA20 particles in a PA-6 matrix are observed and for the blends with less than 35% PA-6, PA-6 particles in a PMMA/SMA20 matrix (*Figure 2*).

It can thus be concluded that the region of phase co-continuity is much smaller in the compatibilised blends and that this region is shifted to lower contents of PA-6. These results are summarised in *Figure 3*, together with the data related to the blends with lower molecular weight PA-6. The narrowing of the region of phase co-continuity can be understood on the basis of the reduced rate of coalescence in the compatibilised blends. The phenomenon of coalescence was discussed in Part 1 of this series of papers[3]. The higher rate of coalescence in non-compatibilised blends is expected to result much easier in a co-continuous phase morphology. It is more difficult to explain the shift of the co-continuous region due to compatibilisation. The following factors have to be taken into account. Firstly, due to the covalent bonding of the two phases at their interface, the viscosity of the blend and the mobility of the phases will be altered. Secondly, in reactively compatibilised blends a very thick interface (up to 50 nm; see Part 3[16]) between the phases is formed which can be considered as a third phase (core/shell structure of the dispersed particles). It is quite evident that simple equations, based on the viscosity ratio and the volume ratio of the blend components, will not be able to predict the region of phase inversion in reactively compatibilised blends. Possibly, the shift of the co-continuous region will be different for different systems. As already mentioned, the system PA-6,6/PP did not give rise to a shift of the co-continuous region[10].

In *Figure 3*, the morphology data for the blends with a lower molecular weight PA-6 are presented. The region of phase co-continuity is again quite large for the non-compatibilised blends (from 50 to 30% PA-6). The special kind of morphology consisting of a network of PMMA rods in the direction of the flow is not observed for this blend series. The five blend compositions which were not disintegrated in $CHCl_3$ or in HCl, 6 N, showed a co-continuous phase morphology after using both etching methods. Compared to the blends with a higher molecular weight PA-6, the region of phase co-continuity is shifted to a lower PA-6 content. This was expected because the blend component with the lowest viscosity has the tendency to encapsulate the other component. For the compatibilised blends with the low molecular weight PA-6, only the blend with 25% PA-6 was not disintegrated in $CHCl_3$ or in HCl, 6 N, and is considered to have a co-continuous phase morphology. However, as it was also the case with the higher molecular weight PA-6, neither of the two etching methods really revealed a co-continuous phase morphology.

The melt-viscosity of the different blend components at 240°C, as measured with capillary rheometry, is represented in *Figure 4*. The following equation has been proposed by Jordhamo *et al.*[6] to predict the location of the point of phase inversion in a binary blend:

$$\frac{\eta_1 \cdot \phi_2}{\eta_2 \cdot \phi_1} = 1 \qquad (1)$$

In this equation, η represents the viscosity (Pa·s) and Φ the volume fraction of the components of the binary blend. On the basis of the viscosity data, it is possible to calculate the point of phase inversion for the non-compatibilised blends and to compare it with the experimental results. According to the approximation made by Wu[9] and other authors, the shear rate in the double-screw mini-extruder was estimated

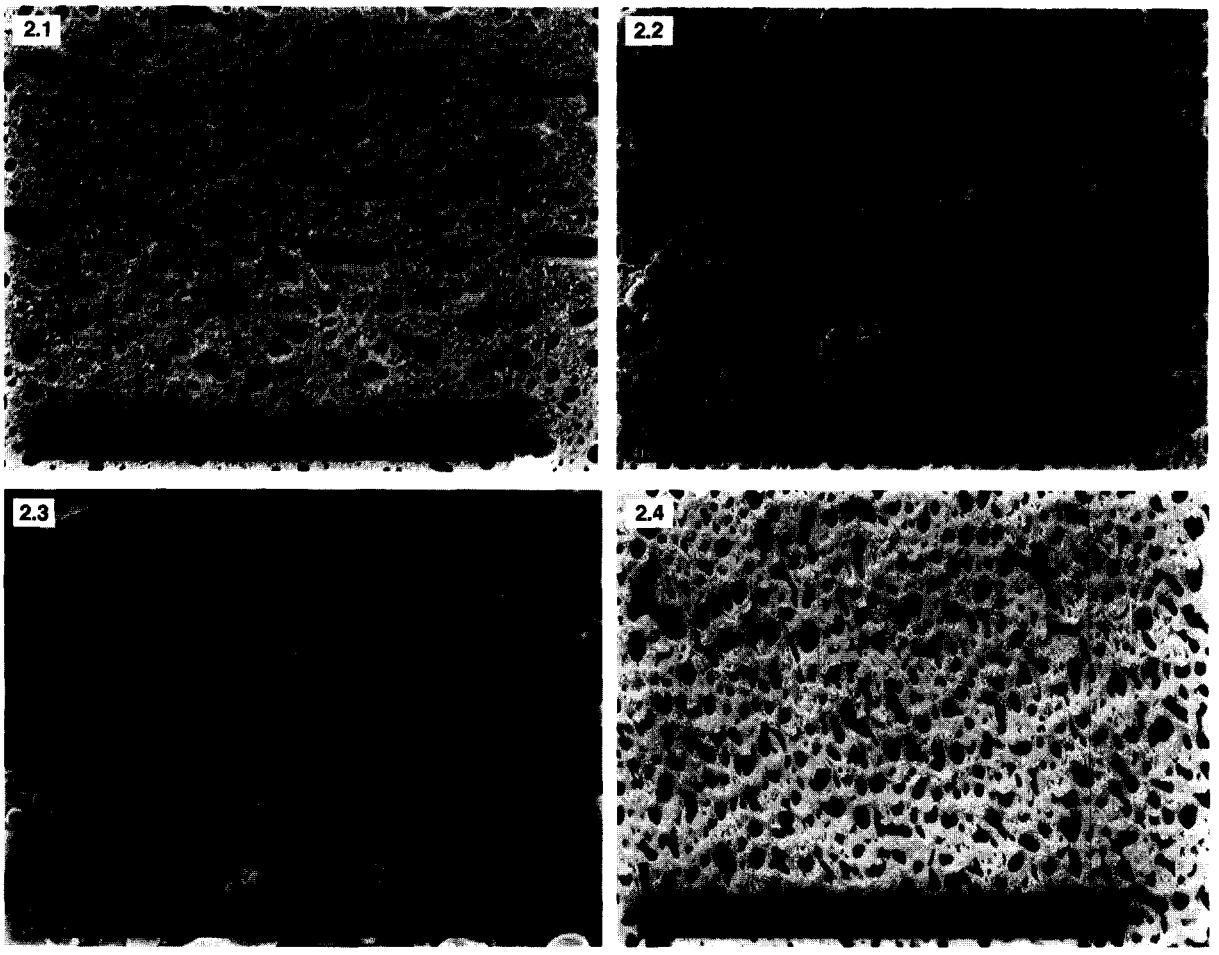

Figure 2 SEM micrographs of the phase morphology of reactively compatibilised PA-6/(PMMA/SMA20) blends. (1) 30% PA-6; (2) 35% PA-6; (3) 35% PA-6; (4) 40% PA-6. (1,2) Etching with HCl, 6 N; (3,4) etching with $CHCl_3$

to be nearly equal to the screw rate (rpm). By this method, the shear rate in the mini-extruder was approximated to be 100 s^{-1}. The composition of phase inversion was calculated to be 24% PA-6 for the lower molecular weight PA-6 and 54% PA-6 for the higher molecular weight PA-6. This prediction is not completely in agreement with the experimental data. The viscosity of the phase PMMA/SMA20 (80/20) was also measured (*Figure 4*); the addition of 20% SMA20 does not alter the viscosity of PMMA.

Morphological stability during annealing

The thermal stability of the different phase morphologies was analysed for the compatibilised and the non-compatibilised blends with the higher molecular weight PA-6. The extruded strands were embedded in an aluminum foil and kept in a vacuum oven at 260°C for 15 min. There was no contact between the sample and a hot metal plate of the oven in order to avoid a selective heating of one of the sides of the extruded polymer strand. The morphology of the compatibilised blends PA-6/(PMMA/SMA20) was not changed after the thermal treatment. For the non-compatibilised blends, the resulting phase morphology of the blends PA-6/PMMA after the thermal treatment is summarised in *Figure 5*. For the blends consisting of a PA-6 matrix and dispersed PMMA particles (% PA-6 > 70%), the particle size was not altered during the annealing. The morphology of the blends PA-6/PMMA with a co-continuous morphology of PMMA rods in the flow direction (70, 65 and 60% PA-6) was affected by the thermal treatment. A disintegration test in HCl (as discussed before) of these annealed

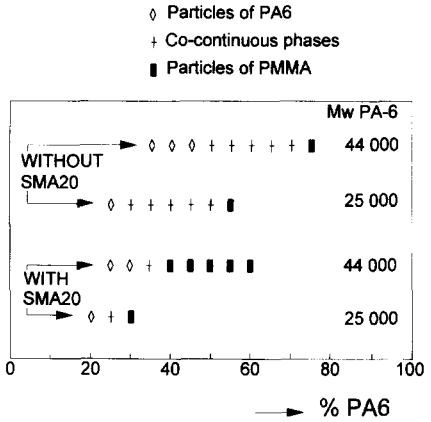

Figure 3 Summary of the phase morphologies of different reactively compatibilised PA-6/(PMMA/SMA20) blends as a function of the PA-6 content

blends resulted in a complete disintegration, while this was not the case before the thermal treatment. This indicates that the co-continuous phase morphology of these blends has changed into a morphology consisting of a matrix of PA-6 with dispersed PMMA particles. The morphology of the other two co-continuous PA-6/PMMA blends (55 and 50% PA-6) was very coarse after the thermal treatment but still co-continuous. The morphology of the PA-6/PMMA blends consisting of PA-6 particles in a PMMA matrix (<50% PA-6) was also drastically changed by the thermal treatment; a very coarse and co-continuous morphology

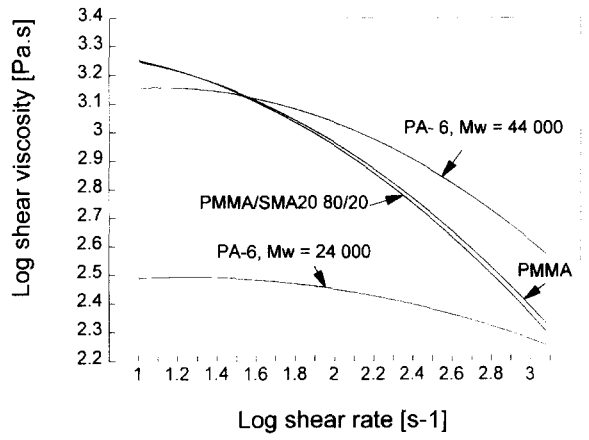

Figure 4 Shear viscosity of the different polymers at 240°C as a function of the shear rate

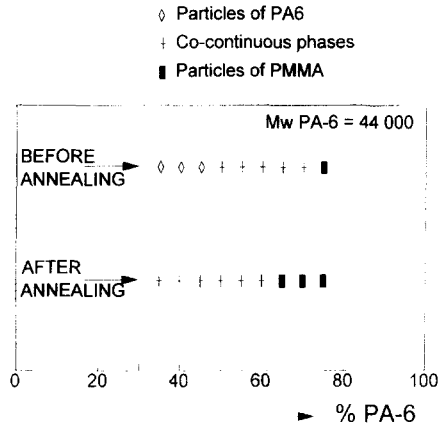

Figure 5 Comparison of the phase morphology of the blend series PA-6/PMMA before and after annealing in the melt

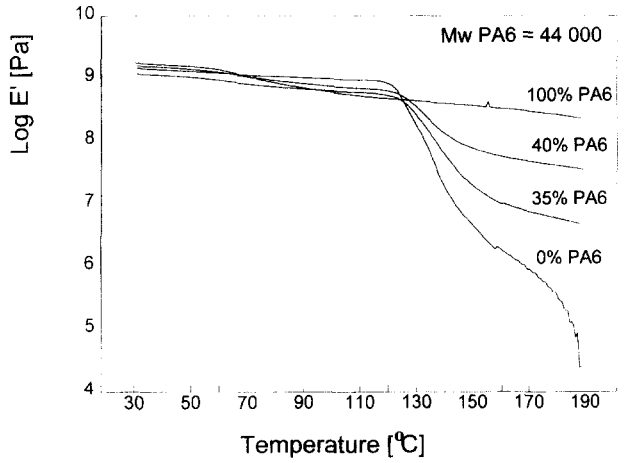

Figure 6 Storage modulus (log E') as a function of the temperature for different blends PA-6/(PMMA/SMA20)

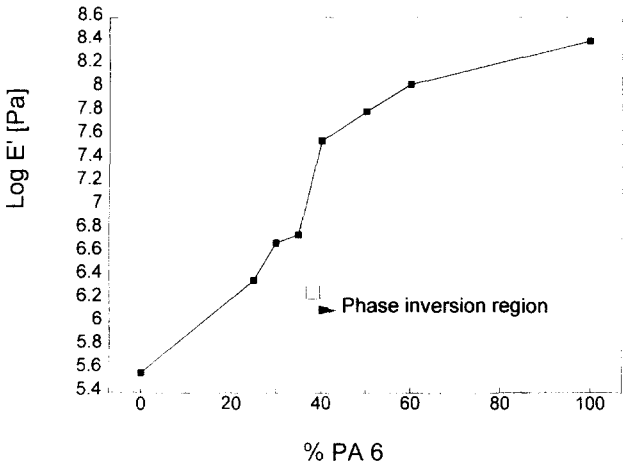

Figure 7 Storage modulus (log E') at 180°C as a function of the PA-6 content in blends PA-6/(PMMA/SMA20)

was observed with SEM. These blends were not disintegrated by $CHCl_3$, nor by HCl after the thermal treatment, which was also an indication for the co-continuous phase morphology. It can be concluded (as seen in *Figure 5*) that the region of co-continuity in PA-6/PMMA blends is shifted to a lower PA-6 content due to the thermal treatment.

Dynamic mechanical behaviour

The aim of this part of the work was to confirm the results obtained with the disintegration tests and with SEM. As dynamic mechanical properties depend mainly on the nature of the matrix, DMTA results should be related to the previous data. Concerning the blend composition with a doubtful phase morphology, some extra information could be obtained.

The dynamic mechanical properties were analysed for the blend series PA-6/(PMMA/SMA20) with the higher molecular weight PA-6. The storage modulus E' as a function of the temperature is presented in *Figure 6* for different blend compositions. The slight decrease of E' at ± 60°C corresponds to the T_g of the amorphous part of PA-6, while the larger decrease of E' at ± 130°C corresponds to the T_g of the amorphous phase PMMA/SMA20. The value of E' at 180°C is plotted as a function of the PA-6 content in *Figure 7*. At the phase inversion point (35% PA-6) of the blends, the value of E' is drastically changed. When the wt% PA-6 in the PA-6/(PMMA/SMA20) blends is higher than 35%, PA-6 forms the matrix. At a temperature of 180°C, PA-6 will still have its solid-state properties because PA-6 is still far below its melting point (221°C), and E' will be relatively high. However, when the wt% PA-6 in the blends is lower than 35%, PMMA/SMA20 will form the matrix. At a temperature of 180°C, the amorphous phase PMMA/SMA20 is far above its T_g and E' will be quite low. The blend with 35% PA-6 was considered as co-continuous on the basis of disintegration tests, but SEM results showed a matrix of PMMA/SMA20 with PA-6 particles. The dynamic mechanical behaviour also indicates that the PMMA/SMA20 phase forms the matrix. The question still remains whether or not the PA-6 particles are connected via a network structure. This will be discussed in the next section.

Tan δ was also analysed for the blends PA-6/(PMMA/SMA20); the results are presented in *Figure 8*. The maximum intensity of the tan δ peak, corresponding to the T_g of the PMMA/SMA20 phase, is very dependent on the matrix type. In *Figure 9*, the maximum of tan δ is plotted as a function of the PA-6 content in the PA-6/(PMMA/SMA20) blends. At the point of phase inversion, the maximum intensity of the tan δ peak is drastically changed; it can also be seen that the maximum of tan δ is shifted to another temperature at the point of phase inversion. For blends with a PA-6 matrix, the maximum of tan δ is found at ± 138°C. For blends with a PMMA matrix, it is found at

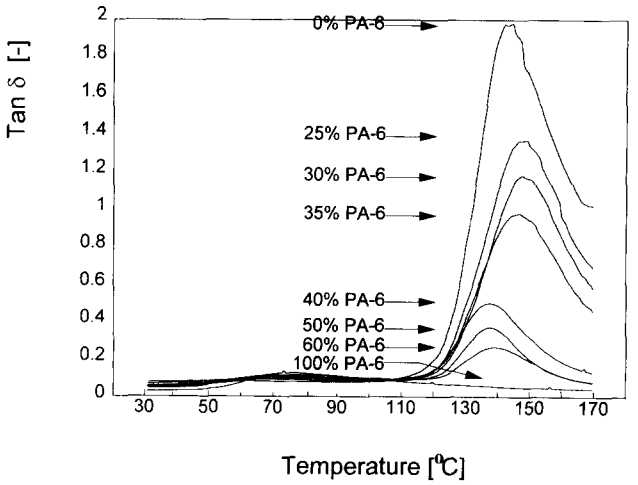

Figure 8 Tan δ as a function of the temperature for different blends PA-6/(PMMA/SMA20)

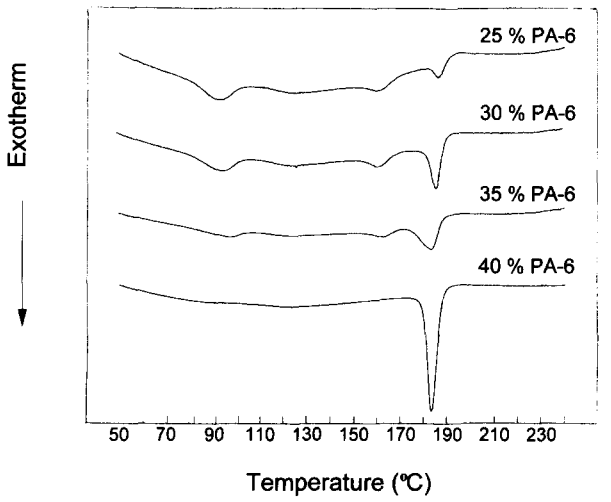

Figure 10 D.s.c. crystallisation curves for compatibilised PA-6/(PMMA/SMA20) blends (M_w PA-6 = 44 000)

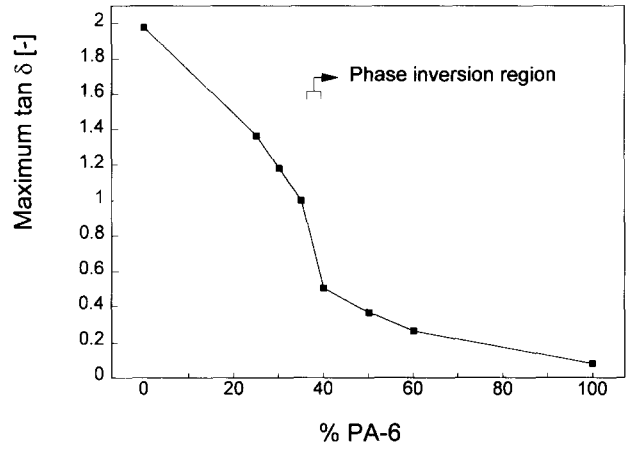

Figure 9 The maximum value of tan δ as a function of the PA-6 content in blends PA-6/(PMMA/SMA20)

±148°C. The reason for this temperature shift is not clear yet.

The morphology of the DMTA bars was also analysed with SEM in order to check if the morphology was changed during the sample preparation. The morphology was not changed for the blends with a PMMA/SMA20 matrix (<40% PA-6). For the blend with 40% PA-6, the morphology tends to become co-continuous in some regions of the DMTA bar; this effect gradually became less important as the % PA-6 increased.

Crystallisation behaviour

In the last experimental part, the relation between the crystallisation behaviour of PA-6 and the phase morphology was studied in order to confirm the previous phase morphology results and eventually to obtain some extra information. The crystallisation behaviour of PA-6 in the compatibilised blends PA-6/(PMMA/SMA20) was analysed with d.s.c. The results are given in *Figure 10* for blends with the higher molecular weight PA-6. All the d.s.c. curves are normalised with respect to the amount of PA-6 in the blends. In *Figure 10*, it can be noticed that only one crystallisation peak is seen for the blends with 40% PA-6; this was also the case for all the blends with a higher amount of PA-6. For all these blends, PA-6 forms the matrix and the crystallisation behaviour is the same as for the pure PA-6. However, several crystallisation exotherms are observed for blends with less than 40% PA-6. This fractionated crystallisation behaviour was also observed by other authors in blend systems where the crystallisable component forms the dispersed phase[17–21]. When the number of heterogeneous nuclei becomes lower than the number of dispersed particles, some particles will not contain heterogeneous nuclei and, as a consequence, will not crystallise at the normal crystallisation temperature. These dispersed particles can eventually possess nuclei which only become active at a lower temperature; this is probably the case for the crystallisation peak observed at 160°C. A third crystallisation peak is observed at ±95°C; the nature of this peak can be due to another kind of nuclei becoming active at this temperature or eventually to homogeneous nucleation.

It is important to note that the presence of the fractionated crystallisation peaks proves the existence of dispersed PA-6 particles. For the blend with 35% PA-6, it can be concluded that a lot of the PA-6 particles (*Figure 2*) are not a part of a co-continuous PA-6 phase network but discrete dispersed PA-6 particles in a PMMA/SMA20 matrix.

The crystallisation behaviour of the blends PA-6/(PMMA/SMA20) with the lower molecular weight PA-6 is presented in *Figure 11*. Fractionated crystallisation is also observed for the blends with dispersed PA-6 particles. For the blend with 25% PA-6, the presence of the fractionated crystallisation peaks again proves the existence of dispersed PA-6 particles.

CONCLUSIONS

The phase inversion in the blend system PA-6/(PMMA/SMA20) was investigated using different techniques. A disintegration test in a selective solvent for one of the blend components is a very suitable method to identify the type of blend phase morphology (matrix particle, co-continuous). Scanning electron microscopy was used to visualise the different blend morphologies, but one should take care in interpreting the morphologies; a two-dimensional view of a co-continuous phase morphology may look like a matrix–particle morphology. The comparison of the morphologies using two different etching methods is very useful. The analysis of the dynamic mechanical properties of the blends confirmed the results obtained with the other techniques but

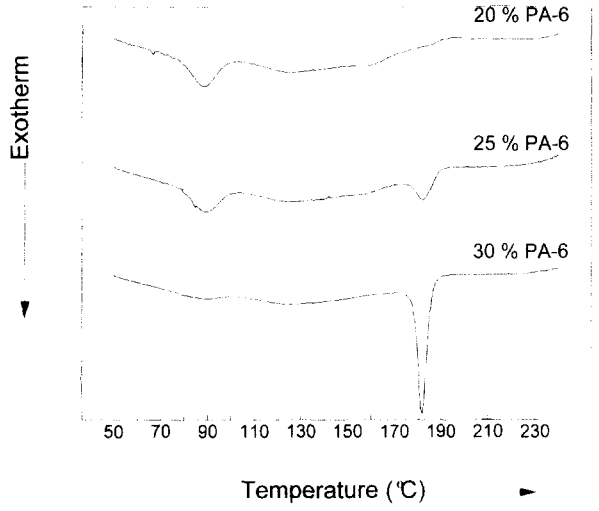

Figure 11 D.s.c. crystallisation curves for compatibilised PA-6/(PMMA/SMA20)blends (M_w PA-6 = 24 000)

provided no additional information. Finally, the presence of different crystallisation peaks for PA-6 during cooling from the melt clearly proved the presence of dispersed PA-6 particles. For some blends, the presence of fractionated crystallisation peaks provides some extra information concerning the phase morphology which could not be obtained by the previous techniques.

For the blend system PA-6/(PMMA/SMA20), the most relevant conclusions can be summarised as follows.

(1) The region of phase co-continuity is quite broad in the non-compatibilised PA-6/PMMA blends. In the compatibilised blends PA-6/(PMMA/SMA20), this co-continuous region is very small. A co-continuous morphology was not observed with SEM for the compatibilised blends.

(2) The point of phase inversion is shifted to a lower PA-6 content in the compatibilised blends. Reactively compatibilised blends are considered to be very complex systems for which the point of phase inversion can not be predicted.

(3) The region of phase co-continuity is shifted to a lower PA-6 content when the molecular weight of PA-6 is decreased; this shift is in agreement with the change in viscosity of PA-6.

ACKNOWLEDGEMENTS

The financial support of the Research Council KU Leuven and the Fund for Scientific Research–Flanders (FWO–Vlaanderen) is gratefully acknowledged. The authors are also indebted to the Flemish Institute I.W.T. for a Ph.D. grant to one of them (K.D.). We are also thankful to the Laboratory of Applied Rheology and Polymer Processing (Prof. P. Moldenaers/Prof. J. Mewis) of the Faculty of Applied Sciences of KULeuven for the melt-viscosity measurements. We are also thankful to Drs. V. Schiepers for her assistance during the experiments.

REFERENCES

1. Xanthos, M., *Polym. Eng. Sci.*, 1988, **28**, 1392.
2. Triacca, V. J., Ziaee, S., Barlow, J. W., Keskkula, H. and Paul, D. R., *Polymer*, 1991, **32**, 1401.
3. Dedecker, K. and Groeninckx, G., *Polymer*, 1998, **39**, 4985.
4. Favis, B. D. and Chalifoux, J. P., *Polymer*, 1988, **29**, 1761.
5. Quintens, D., Groeninckx, G., Guest, M. and Aerts, L., *Polym. Eng. Sci.*, 1990, **30**, 1474.
6. Jordhamo, G. M., Manson, J. A. and Sperling, L. H., *Polym. Eng. Sci.*, 1986, **26**, 517.
7. Favis, B. D. and Willis, J. M., *J. Polym. Sci.: Part B: Polym. Phys.*, 1990, **28**, 2259.
8. Favis, B. D. and Chalifoux, J. P., *Polym. Eng. Sci.*, 1987, **27**, 1591.
9. Wu, S., *Polym. Eng. Sci.*, 1987, **27**, 335.
10. Hietaoja, P. T., Holsti-Miettinen, R. M., Seppälä, J. and Ikkala, O. T., *J. Appl. Polym. Sci.*, 1994, **54**, 1613.
11. Maréchal, Ph., Legras, R. and Deconinck, J. M., *J. Polym. Sci.: Part A: Polym. Chem.*, 1993, **31**, 2057.
12. Song, J., Fischer, H. and Schnabel, W., *Polymer Degradation Stability*, 1992, **36**, 261.
13. Paul, D. R. and Barlow, J. W., *Polymer*, 1984, **25**, 487.
14. Brannock, G. R., Barlow, J. W. and Paul, D. R., *J. Polym. Sci.: Part B: Polym. Phys.*, 1991, **29**, 413.
15. Chen, D. and Kennedy, J. P., *Polym. Bull.*, 1987, **17**, 71.
16. Dedecker, K. and Groeninckx, G., *Polymer*, 1998, **39**, 5001.
17. Moon, H., Ryoo, B. and Park, J., *J. Polym. Sci., Part B: Polym. Phys.*, 1994, **32**, 1427.
18. Tang, T. and Huang, B., *J. Appl. Polym. Sci.*, 1994, **53**, 355.
19. Tang, T. and Huang, B., *J. Polym. Sci., Part B: Polym. Phys.*, 1994, **32**, 1991.
20. Everaert, V. and Groeninckx, G., *Extended Abstracts of the European Symposium on Polymer Blends*, Maastricht, The Netherlands, 1996, p. 111.
21. Mischenko, N., Groeninckx, G., Reynaers, H., Koch, M. and Pracella, M., Abstract, in the *4th ATM Conference on Advanced Topics in Polymer Science*, Gargnano, Italy, 1996, p. 46.